



1 **Old Carbon, New Insights: Thermal Reactivity and Bioavailability of Saltmarsh Soils**

2 Alex Houston¹, Mark H Garnett², Jo Smith³, and William E N Austin^{1,4}

3 1. Department of Geography and Sustainable Development, University of St Andrews, St
4 Andrews, KY16 9AL, United Kingdom

5 2. NEIF Radiocarbon Laboratory, Scottish Universities Environmental Research Centre, East
6 Kilbride, G75 0QF, United Kingdom

7 3. Institute of Biological & Environmental Sciences, School of Biological Science, University of
8 Aberdeen, Aberdeen, AB24 3FX, United Kingdom

9 4. Scottish Association of Marine Science, Oban, PA37 1QA, United Kingdom

10 *Correspondence to:* Alex Houston (ah383@st-andrews.ac.uk)

11 **Abstract**

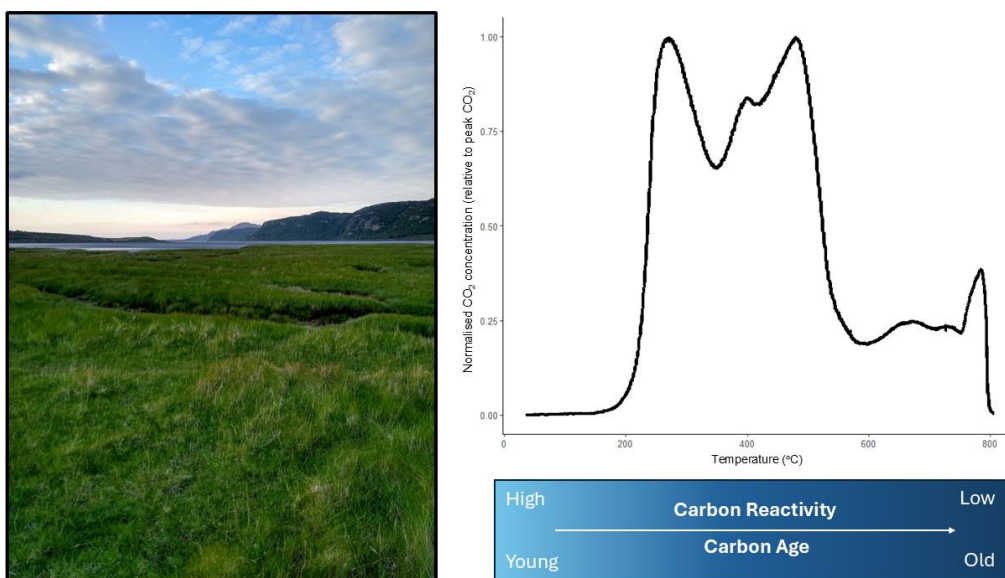
12 Saltmarshes are globally important coastal wetlands which can store carbon for millennia, helping
13 to mitigate the impacts of climate change. They accumulate organic carbon from both
14 autochthonous sources (above- and belowground plant production) and allochthonous sources
15 (terrestrial and marine sediments deposited during tidal inundation). Previous studies have found
16 that long-term organic carbon storage in saltmarsh soils is driven by the pre-aged allochthonous
17 fraction, implying that autochthonous organic carbon is recycled at a faster rate. However, it is also
18 acknowledged that the bioavailability of soil organic carbon depends as much upon environmental
19 conditions as the reactivity of the organic carbon itself. Until now, there has been no empirical
20 evidence linking the reactivity of saltmarsh soil organic carbon with its bioavailability for
21 remineralization.

22 We found that the ¹⁴C age of CO₂ produced during ramped oxidation of soils from the same saltmarsh
23 ranged from 201 to 14,875 years BP, and that ¹⁴C-depleted (older) carbon evolved from higher
24 temperature ramped oxidation fractions, indicating that older carbon dominates the thermally
25 recalcitrant fractions. In most cases, the ¹⁴C content of the lowest temperature ramped oxidation
26 fraction (the most thermally labile organic C source) was closest to the previously reported ¹⁴C
27 content of the CO₂ evolved from aerobic incubations of the same soils, implying that the latter was
28 from a thermally labile organic carbon source. This implies that the bioavailability of saltmarsh soil
29 organic carbon to remineralisation in oxic conditions is closely related to its thermal reactivity.



30 Management interventions (e.g. rewetting by tidal inundation) to limit the exposure of saltmarsh soils
31 to elevated oxygen availability may help to protect and conserve these stores of old, labile organic
32 carbon and hence limit CO₂ emissions.

33 Graphical Abstract



34

35 1. Introduction

36 Saltmarshes accumulate organic carbon (OC) of variable age and reactivity into their soils. A portion
37 of this OC is stored for millennia, providing a climate regulation service, and some is returned to the
38 atmosphere or laterally exported (Komada et al., 2022; Macreadie et al., 2021). Saltmarshes also
39 accumulate and produce inorganic carbon (IC) but the climate regulation service of this is currently
40 under debate and unclear (Granse et al., 2024; Van Dam et al., 2021).

41 To understand the role of saltmarsh soils in carbon cycling and their potential for climate mitigation
42 through targeted management interventions, much research has focussed on determining the
43 autochthonous (in-situ) and allochthonous (ex-situ, trapped during tidal inundation from terrestrial
44 and marine sources) contributions to saltmarsh soils, with the accumulation of autochthonous OC
45 a direct sequestration of carbon from the atmosphere, reducing the amount of atmospheric
46 greenhouse gases (GHGs) (Macreadie et al., 2019; Saintilan et al., 2013; Van de Broek et al., 2018).



47 The accumulation of allochthonous OC, originally sequestered outside the saltmarsh area, does not
48 directly reduce atmospheric GHGs, but can represent a source of avoided emissions if it remains
49 stored in the saltmarsh soil for longer than in an alternative depositional environment (Howard et al.,
50 2023). Evidence to determine whether this is the case or not, and under what scenarios, has proven
51 challenging to obtain (Houston et al., 2024).

52 Another approach is to partition the saltmarsh soil OC pool by reactivity (Luk et al., 2021), which may
53 provide greater insight into the soil carbon residence time and therefore the climate mitigation
54 achieved through targeted management interventions (Sanderman and Grandy, 2020). Soil OC
55 reactivity can be defined as its availability for remineralisation by soil microbial communities, with
56 different reactivity pools having different turnover times (Plante et al., 2009).

57 The proportions of autochthonous and allochthonous OC accumulating in saltmarsh soils and OC
58 reactivity pools are thought to be related, as in-situ processes during burial of saltmarsh soils have
59 been suggested to favour the long-term storage of aged, allochthonous OC (Komada et al., 2022;
60 Leorri et al., 2018; Mueller et al., 2019; Van de Broek et al., 2018). Young OC, which can be
61 autochthonous or allochthonous (Van de Broek et al., 2018), is hypothesised to turnover at a faster
62 rate, often resulting in its remineralisation to the atmosphere. It is therefore assumed that old OC is
63 mostly composed of recalcitrant (low reactivity) components, whereas young OC contains a greater
64 proportion of labile (reactive) components (Komada et al., 2022; Van de Broek et al., 2018). Of
65 course, this is not always the case as young OC can contain recalcitrant material, and older OC can
66 be labile if it was stored in a stable environment with low carbon turnover rates, such as a permafrost
67 soil, prior to its mobilisation (Dasari et al., 2024).

68 Houston et al. (2024) found that a portion of the carbon dioxide (CO₂) evolved during aerobic
69 incubations of saltmarsh soils was from an old, allochthonous source. It is possible that the CO₂
70 could have been evolved from a labile source, or a physically stabilized source that decomposed due
71 to increased oxygen availability (a thermodynamically favourable terminal electron acceptor
72 facilitating the degradation of OC which was stable in a low-oxygen environment, as saltmarsh soils
73 typically are (Noyce et al., 2023)). To constrain these sources, the ¹⁴C composition of the biologically
74 evolved CO₂ from these experiments can be directly compared to the ¹⁴C composition of the
75 thermally characterized soil OC.



76 The thermal reactivity of soil OC can usefully be approximated using ramped oxidation (RO), which
77 involves measuring the quantity of CO₂ evolved as a sample is increasingly heated at a constant rate
78 in an atmosphere containing oxygen (Garnett et al., 2023). The energy required to thermally-evolve
79 CO₂ is expected to be related to the energy required for biological degradation of OC, with CO₂
80 evolved at low temperatures deemed to be from more reactive soil OC pools than CO₂ evolved at
81 higher temperatures (Peltre et al., 2013). The age of the OC reactivity pools can be examined by
82 collecting the evolved CO₂ from set temperature ranges and measuring the ¹⁴C (age) content (Garnett
83 et al., 2023; Plante et al., 2013). These can be compared to the ¹⁴C content of the CO₂ that is evolved
84 biologically during incubations of equivalent samples to determine whether the age of the most
85 biologically- and thermally-reactive OC pools match, or not (Plante et al., 2011).

86 The ¹⁴C content of the thermal reactivity pools also provides insight into the turnover time of each
87 pool, with past research showing that the oldest soil organic matter (OM) (most depleted ¹⁴C content)
88 tends to dominate the most thermally stable fractions (Bao et al., 2019; Plante et al., 2013; Stoner et
89 al., 2023). Similar results have been found for saltmarsh soils (Luk et al., 2021). The ¹³C content of
90 the thermal reactivity pools can also provide insight as to whether the source of OC has an influence
91 on turnover time. Previous work shows that the ¹³C content of evolved CO₂ tends to be more enriched
92 at higher temperatures due to greater contributions from ¹³C-enriched, degraded/microbially derived
93 C (Luk et al., 2021; Sanderman and Grandy, 2020; Stoner et al., 2023).

94 Here, we present the first measurements of the ¹³C and ¹⁴C content of CO₂ derived from saltmarsh
95 soils using ramped oxidation, and the first comparison of these to the ¹⁴C content of biologically
96 evolved CO₂ from the same soils (Houston et al., 2024). We hypothesised that the pre-aged,
97 allochthonous CO₂ respired from saltmarsh soils in Houston et al. (2024) was from a thermally labile
98 source, and that the thermally recalcitrant OC pools would be predominantly composed of older OC.

99 2. Methods

100 **2.1. Field site and sample collection:** Three saltmarsh soil cores (T1-3) were retrieved ca. 30 m
101 apart from the lower marsh zone from Skinflats (SK), an estuarine saltmarsh in Scotland (56°
102 3'34.04"N, 3°43'59.16"W), as detailed in Houston et al. (2024). Field methods and laboratory sub-
103 sampling procedures are described in detail in Houston et al. (2024). Briefly, the cores were split into
104 1 cm thick slices as follows: core T1 (0-1 cm, 5-6 cm, and 18-19 cm); T2 (0-1 cm, 5-6 cm, and 15-16
105 cm), and T3 (0-1 cm, 5-6 cm, and 19-20 cm) (with the deepest sample from each core being the



106 deepest retrieved sample). Each slice was subsequently divided to provide sample material for the
107 RO procedure, and for aerobic laboratory incubations from which the biologically evolved CO₂ was
108 collected for ¹³C and ¹⁴C analysis (Houston et al., 2024).

109 **2.2. Ramped oxidation:** The RO sub-samples were individually dried to constant mass before milling
110 to a fine powder to homogenise and limit potential shielding effects from aggregates. The samples
111 were then sent to the NEIF Radiocarbon Laboratory for the RO procedure, which is described in
112 Garnett et al. (2023). In brief, the samples were progressively heated at a constant rate of 5°C per
113 minute from ambient room temperature to 800°C in a stream of high purity oxygen and the evolved
114 CO₂ measured. Temperature ranges, which defined OC reactivity pools, were identified from the
115 resulting thermograms: 150-325°C (t1), 325- 425°C (t2), 425-500°C (t3), 500-650°C (t4), and 650-
116 800°C (t5). The RO procedure was then re-run with new sample material and the thermally evolved
117 CO₂ collected for ¹³C and ¹⁴C analyses from the pre-defined temperature increments. The ¹³C and ¹⁴C
118 analyses of these CO₂ samples followed the same methodology at the same laboratory as in Houston
119 et al. (2024). Briefly, following cryogenic purification, the recovered sample CO₂ was graphitised and
120 analysed for ¹⁴C content at the Scottish Universities Environmental Research Centre Accelerator
121 Mass Spectrometry (AMS) Laboratory. A sub-sample of the recovered CO₂ was analysed for ¹³C
122 content (δ¹³C-VPDB) using isotope ratio mass spectrometry (Thermo-Fisher Delta V, Germany) and
123 used to normalise the ¹⁴C results to a δ¹³C of -25 ‰ to correct for isotopic fractionation. Following
124 convention, ¹⁴C results are presented as %Modern (fraction modern x 100) and conventional
125 radiocarbon ages (years BP, where 0 BP = AD 1950 and age = -8033 x Ln (%Modern/100)).

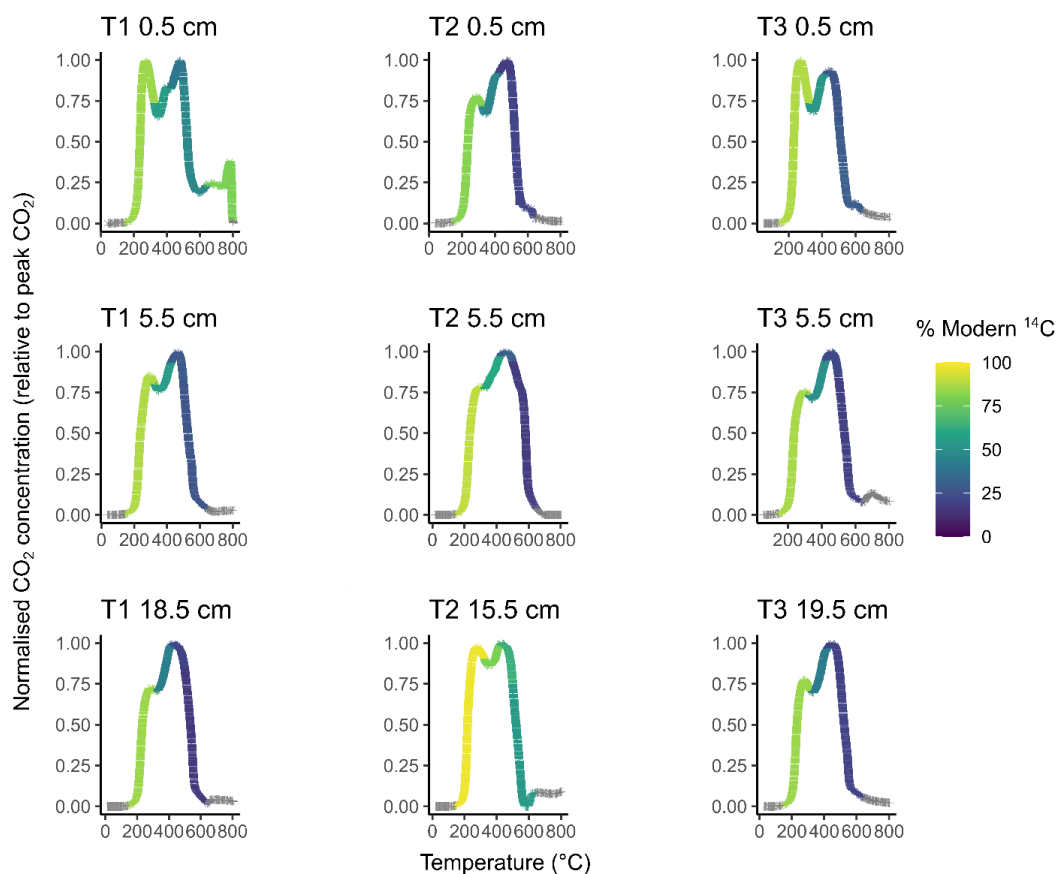
126 **3. Results**

127 **3.1. Thermograms**

128 The CO₂ evolved from the RO analysis had bimodal distributions for most samples, with the major
129 peaks occurring at approximately 250°C and 450°C (Fig. 1). These peaks were within t1 (150-325°C)
130 and t3 (425-500°C), respectively. We calculated the proportion of CO₂ evolved from the lower
131 temperature CO₂ peak (150-425°C; t1 and t2 combined) and the proportion of CO₂ evolved from the
132 higher temperature CO₂ peak (425-650°C; t3 and t4 combined) (Table A1). There were no significant
133 trends with depth for either T1, T2, or T3 (spearman's rho, p > 0.05). Visually, for both T1 and T3 the
134 size of the second major peak relative to the lower temperature peak increased with depth, whereas
135 for T2 the opposite was the case (Fig. 1).



136 Most of the samples showed similar trends for CO₂ produced during the ramped combustion
137 procedure, with a lesser CO₂ peak (t2, 325-425°C) between the two larger peaks of t1 and t3 (Fig. 1,
138 see graphical abstract for magnified example). Following the t3 peak (425-500°C) there was another
139 smaller peak in CO₂ evolution between 500-650°C (t4) (Fig. 1). T1 0.5 cm and T3 5.5 cm had high
140 temperature CO₂ peaks between 650-800°C, but this peak was not present for most of the samples
141 (Fig. 1).



142

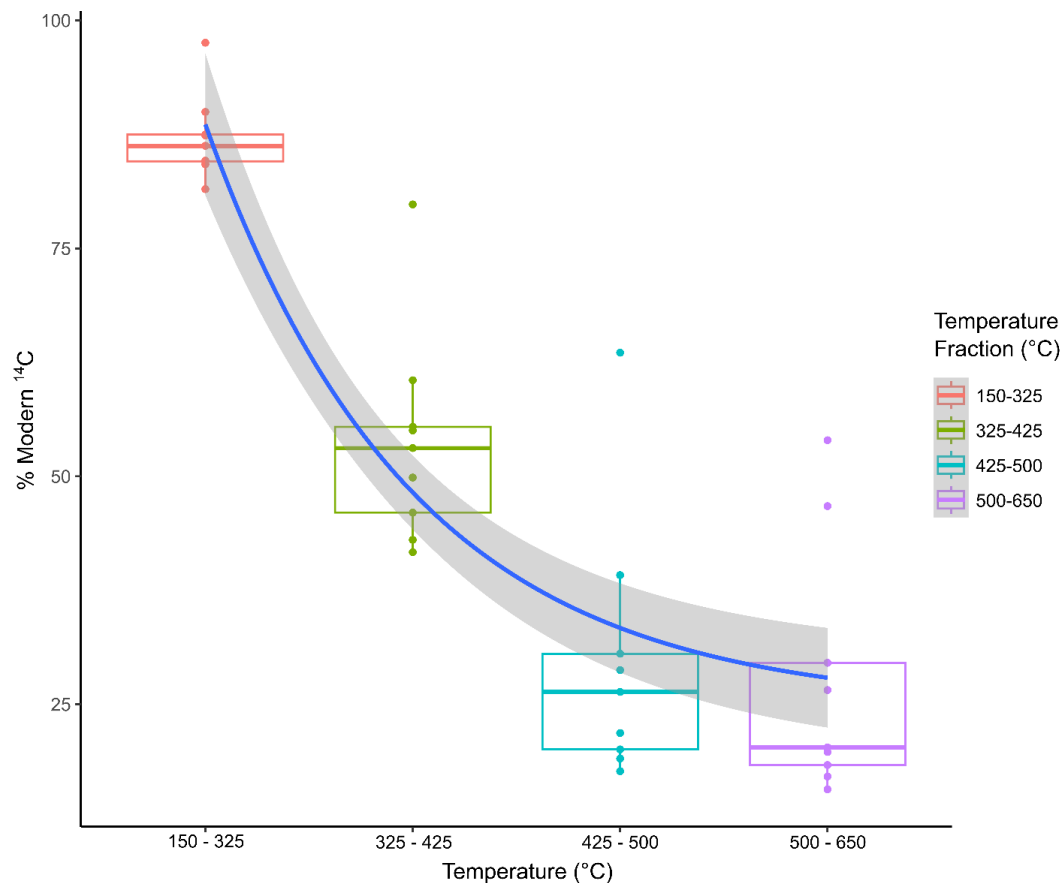
143 *Figure 1. Thermograms for each of the soil samples. The shading colour indicates the % Modern ¹⁴C content of the CO₂*
144 *evolved throughout the ramped oxidation from temperature fractions 150-325°C, 325-425°C, 425-500°, 500-650°C (and*
145 *650-800°C for T1 0.5 cm only). Grey shading indicates values outside of the CO₂ collection range (150-800°C).*

146



147 **3.2. ¹⁴C content of ramped oxidation fractions.**

148 The ¹⁴C content of the CO₂ evolved during the ramped oxidation (¹⁴C-RO) decreased exponentially
149 from 150-650°C (t1-t4) ($p < 0.001$, Fig. 2, Table 1). This regression was calculated using the mid-point
150 of each temperature range (e.g., t1 mid-point is 237.5°C). Sufficient CO₂ for ¹⁴C analysis for 650-
151 800°C (t5) was only recovered from one sample (T1 0.5 cm, Fig. 1, Table 1). This sample did not follow
152 the same decreasing trend in ¹⁴C content with increasing temperature, as it contained a greater
153 amount of ¹⁴C (79.75 ± 0.37 % Modern) than t2, t3 and t4 (39.18 – 55.02 % Modern) (Fig. 1, Table 1).



154

155 *Figure 2. Radiocarbon concentration (% Modern) of the CO₂ evolved from each temperature window during RO (150-325°C,*
156 *325-425°C, 425-500°C, 500-650°C). The blue line is the exponential regression between temperature and ¹⁴C content ($y =$*
157 *$215.76e^{-0.004x}$, $p < 0.001$, $R_2 = 0.77$, $SE = 1.86$, $n = 36$). The grey shading is the 95 % confidence interval of the regression.*

158 For the entire sample set, the ¹⁴C content of the evolved CO₂ ranged from 97.53 ± 0.50 % Modern for
159 T2 15.5 cm (201 ± 41 years BP) to 15.70 ± 0.12 % Modern for T1 18.5 cm ($14,875 \pm 61$ years BP) (Fig.



160 2, Table 1, Table A2). There were no significant trends in ^{14}C content with depth, for example the ^{14}C
 161 contents of the CO_2 evolved from the 150-325°C fraction for the deepest layer (T1 18.5 cm, T2 15.5
 162 cm, T3 19.5 cm), ranged from 84-97 % Modern (1,347-201 years BP), whereas in the surface (0.5 cm)
 163 samples it ranged from 81-87 % Modern (1,643-1,085 years BP) (Table 1, Table A2). The CO_2 evolved
 164 from the 500-650°C fraction for the deepest layer (T1 18.5 cm, T2 15.5 cm, T3 19.5 cm), ranged from
 165 15-54 % Modern (14,875-4,956 years BP), whereas in the surface (0.5 cm) samples it ranged from 20-
 166 47 % Modern (12,826-6,108 years BP) (Table 1, Table A2).

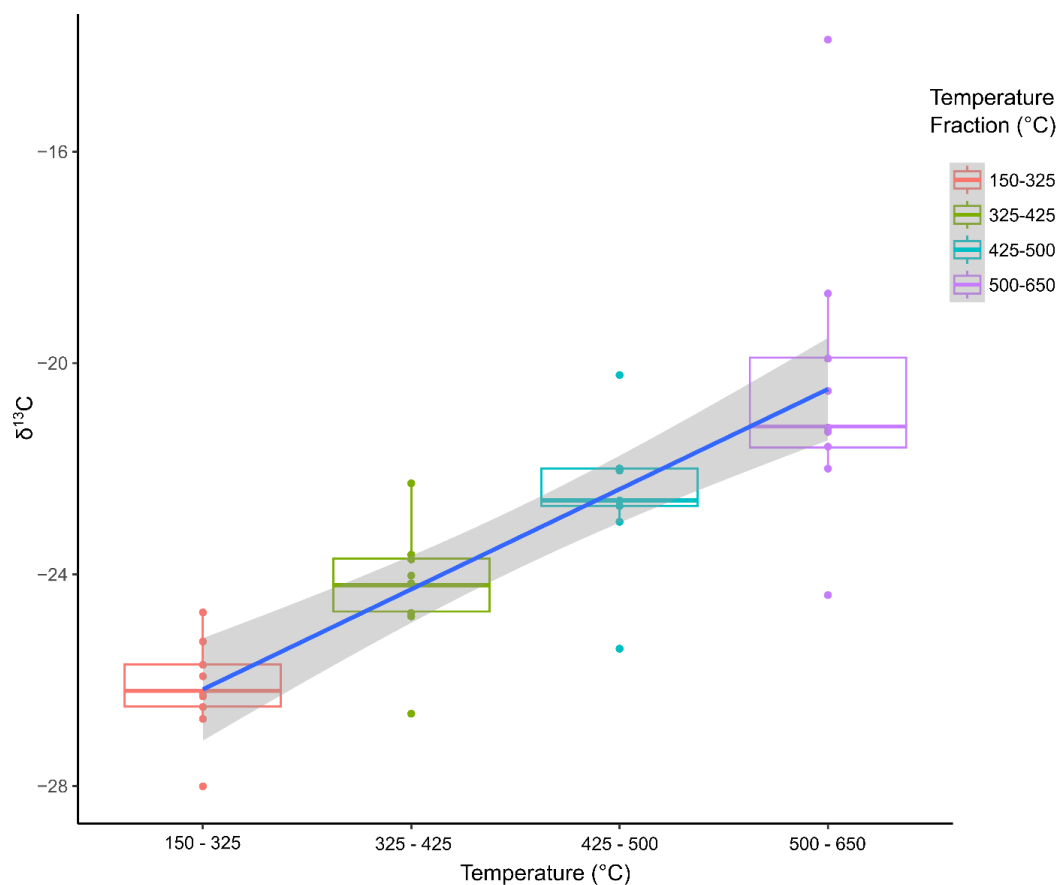
167 *Table 1. Radiocarbon concentration (% Modern) of the CO_2 evolved from each RO temperature fraction and the incubation*
 168 *experiments in Houston et al. (2024).*

	% Modern ^{14}C					Incubations (Houston et al., 2024)
	150-325°C	325-425°C	425-500°C	500-650°C	650-800°C	
T1 0.5 cm	84.62 ± 0.44	55.02 ± 0.29	39.18 ± 0.21	46.75 ± 0.26	79.75 ± 0.37	99.15 ± 0.45
T1 5.5 cm	87.51 ± 0.43	55.43 ± 0.28	28.76 ± 0.17	26.56 ± 0.16		87.18 ± 0.38
T1 18.5 cm	84.56 ± 0.44	43.06 ± 0.23	20.07 ± 0.13	15.70 ± 0.12		36.13 ± 0.36
T2 0.5 cm	81.50 ± 0.43	46.04 ± 0.24	17.67 ± 0.013	20.26 ± 0.14		98.97 ± 0.43
T2 5.5 cm	89.95 ± 0.42	60.55 ± 0.30	30.54 ± 0.17	17.11 ± 0.12		90.26 ± 0.40
T2 15.5 cm	97.53 ± 0.50	79.80 ± 0.41	63.56 ± 0.31	53.96 ± 0.27		94.86 ± 0.44
T3 0.5 cm	87.37 ± 0.45	53.09 ± 0.28	26.37 ± 0.15	29.55 ± 0.17		97.56 ± 0.43
T3 5.5 cm	86.23 ± 0.42	49.86 ± 25	21.87 ± 0.14	18.36 ± 0.12		88.22 ± 0.41
T3 19.5 cm	84.23 ± 0.41	41.67 ± 0.22	19.04 ± 0.13	19.76 ± 0.14		28.25 ± 0.37

169

170 3.3. ^{13}C content of ramped oxidation fractions

171 There was a positive linear relationship between the ^{13}C content of the evolved CO_2 (^{13}C -RO) and
 172 temperature from the RO analysis between 150-650°C ($p < 0.001$, Fig. 3). As for Fig. 2, this regression
 173 was calculated using the mid-point of each temperature range (e.g., t1 mid-point is 237.5°C).



174

175 *Figure 3. ¹³C content of the CO₂ evolved from each temperature window during RO (150-325°C, 325-425°C, 425-500°, 500-*
 176 *650°C). The blue line is the linear regression between temperature and ¹³C content ($y = 0.017x - 30.39$, $p < 0.001$, $R_2 = 0.62$,*
 177 *SE = 1.72, n = 45). The grey shading is the 95 % confidence interval of the regression.*

178 ¹³C values of the RO temperature fractions ranged from -28.0 ‰ to -4.0 ‰ (Table 2). Values for 150-
 179 650°C (t1-t4), the range at which ¹⁴C was also measured (except for one ¹⁴C measurement from the
 180 650-800°C fraction for T1 0.5 cm) ranged from -28.0 ‰ to -13.9 ‰ (Fig. 3, Table 2), and values for
 181 650-800°C fraction (t5) ranged from -21.1 ‰ to -4.0 ‰ (Table 2).

182 *Table 2. δ¹³C-VPDB‰ for the CO₂ evolved from each RO temperature fraction and the incubation experiments in Houston*
 183 *et al. (2024).*

δ¹³C-VPDB‰					
150-325°C	325-425°C	425-500°C	500-650°C	650-800°C	Incubations

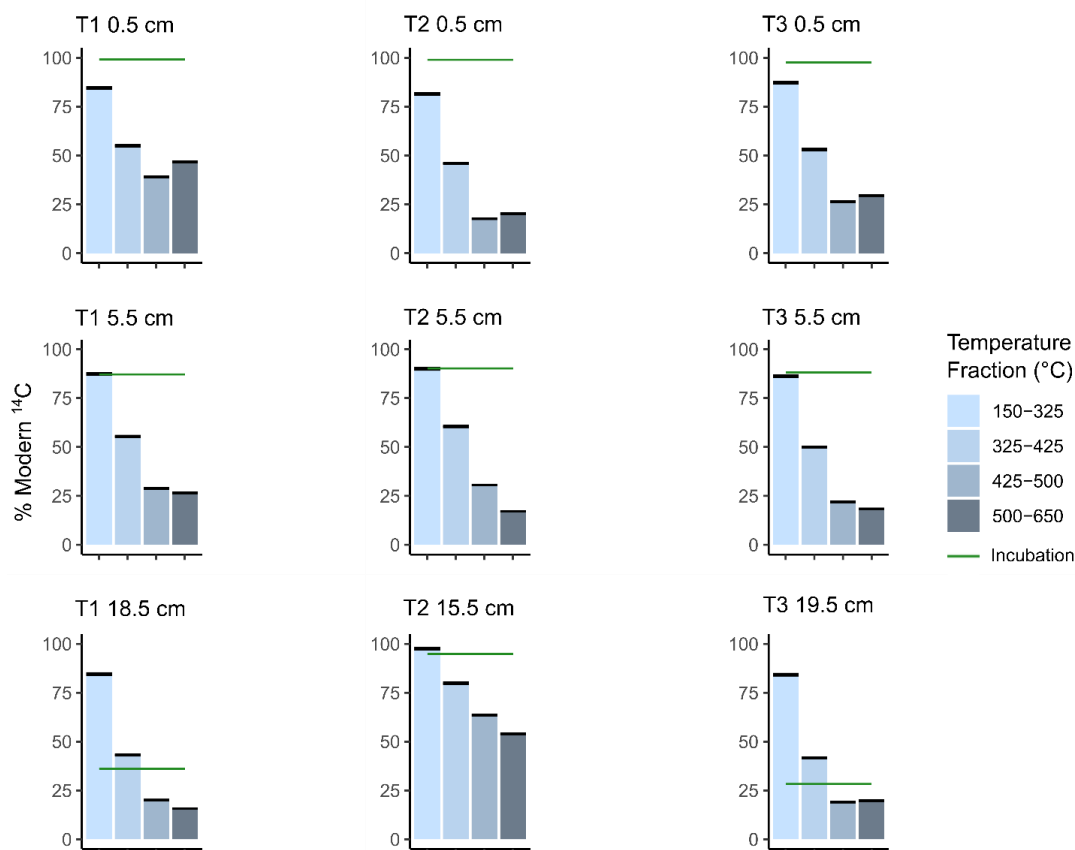


T1 0.5 cm	-24.7	-22.3	-20.2	-13.9	-5.6	-23.3
T1 0.5 cm	-26.7	-24.7	-22.7	-21.3	-6.3	-23.6
T1 18.5 cm	-25.9	-24.0	-22.6	-21.6	-9.5	-6.1
T2 0.5 cm	-25.7	-23.6	-22.0	-19.9	-4.7	-22.9
T2 5.5 cm	-26.5	-24.8	-23.0	-22.0	-21.1	-23.1
T2 15.5 cm	-28.0	-26.6	-25.4	-24.4	-4.0	-20.2
T3 0.5 cm	-25.3	-23.7	-22.0	-18.7	-4.1	-20.6
T3 5.5 cm	-26.2	-24.2	-22.6	-20.5	-12.6	-23.4
T3 19.5 cm	-26.3	-24.2	-22.6	-21.2	-8.0	-3.7

184

185 **3.4. Ramped oxidation and incubation comparison**

186 Figure 4 presents a comparison of the ^{14}C content of the CO_2 evolved from RO temperature fractions
187 (this study) and respired from the same soils during aerobic laboratory incubations (Houston et al.
188 2024). These comparisons show that for each of the 0.5 cm depth samples, the ^{14}C content of the
189 respired CO_2 was greater than the ^{14}C content of the CO_2 evolved from the same soils in any of the
190 RO temperature fractions (Fig. 4). For the 5.5 cm depth samples, the ^{14}C content of the CO_2 respired
191 in the incubations was approximately equivalent to the ^{14}C content of the CO_2 evolved from the 150-
192 325°C RO temperature fraction (Fig. 4). For T2 15.5 cm, the ^{14}C content of the respired CO_2 was also
193 closest to the 150-325°C RO temperature fraction (Fig. 4). For the T1 18.5 cm and T3 19.5 cm
194 samples, the ^{14}C contents of the incubation CO_2 were depleted relative to the 150-325°C RO
195 temperature fraction for both samples, and instead, were closest to the 325-425°C and 425-500°C
196 RO temperature fractions, respectively (Fig. 4)



197

198 *Figure 4. Radiocarbon content (% Modern) of the CO₂ evolved from each temperature window during RO ((150-325°C, 325-*
199 *425°C, 425-500°, 500-650°C. Blue bars) and incubation experiments (green lines, from Houston et al. (2024)).*

200 **4. Discussion**

201 **4.1. Thermograms**

202 During ramped combustion, CO₂ evolved at low temperatures is deemed to be more energetically
203 favourable for decomposition than CO₂ evolved at higher temperatures, implying that the reactivity
204 of soil OC decreases with increasing temperature (Peltre et al., 2013; Williams and Plante, 2018).
205 Due to the approximately bimodal thermogram distribution (Fig. 1), we can therefore define the low-
206 temperature CO₂ peak as relatively 'labile' and the higher temperature CO₂ peak as 'recalcitrant' OC
207 pools (Capel et al., 2006). There were no significant trends between the proportion of CO₂ evolved
208 from the labile (150-425°C) and recalcitrant (425-650°C) RO fractions for either T1, T2, or T3



209 (Spearman's rho, $p > 0.05$), limiting what we can infer from the distributions of the thermograms.
210 Despite the lack of statistical significance, for both T1 and T3 the height of the higher temperature
211 (recalcitrant) peak relative to the lower temperature (labile) peak increases with increasing depth.
212 This may be caused by OM degradation throughout the burial process during which microbes
213 degrade soil OM, and preferentially deplete the labile OM pool as more favourable for
214 decomposition, which in turn can result in deeper soils having greater proportions of recalcitrant,
215 microbially derived OC (Luk et al., 2021; Soldatova et al., 2024).

216 Conversely, for T2 the height of the labile peak increased relative to the recalcitrant peak with
217 increasing depth (Fig. 1). This is likely to be because, as well as the soil burial process and the
218 degradation of OM, all samples were within the soil rooting zone (0-40 cm), which can facilitate the
219 transfer of labile OM from the surface to deep soils (Bernal et al., 2017; Rumpel and Kögel-Knabner,
220 2011). This process may highlight heterogeneity in these saltmarsh soils and in this case may have
221 introduced new labile OM to the deeper soil samples, which was subsequently captured by the RO
222 procedure for the T2 15.5 cm sample, resulting in the increased labile fraction with depth in core T2
223 (15.5 cm). Due to the low-oxygen conditions in waterlogged saltmarsh soils, decomposition rates are
224 slow, and labile OM can persist for extended time periods compared to aerobic soils (Chapman et
225 al., 2019; McTigue et al., 2021). Hence, it is also feasible that the greater proportion of labile OC at
226 depth for T2 is due to preservation of larger inputs of labile OM compounds at the soil surface during
227 the burial process. The difference in the thermogram distributions with depth between T2, and T1/T3,
228 may highlight heterogeneity across the Skinflats saltmarsh soils, even within the same lower marsh
229 zone.

230 **4.2. ^{14}C content of ramped oxidation CO_2 fractions**

231 The changes with depth between the thermogram CO_2 peaks follow similar trends to the RO- ^{14}C
232 content of the corresponding temperature fractions (Fig. 1, Table 1). For T1 and T3, the increasing
233 proportion of evolved CO_2 associated with the recalcitrant (high temperature) peak corresponds to a
234 decrease in RO- ^{14}C content (Fig. 1), i.e., the increase in the amount of CO_2 evolved from a recalcitrant
235 pool corresponds to an increase in its age. For T2, the opposite is observed; the decreasing
236 proportion of the evolved CO_2 associated with the recalcitrant (high temperature) peak corresponds
237 to an increase in RO- ^{14}C content (Fig. 1), i.e., the increase in the amount of CO_2 evolved from the
238 recalcitrant pool corresponds to a decrease in its age. This may suggest the input of a different source
239 of younger but recalcitrant (allochthonous) material in T2. As saltmarsh soil accumulates, and OC is



240 buried and degraded, our data show that the proportion of aged, recalcitrant OC tends to increase
241 with depth, while comparatively younger, labile OC pools also persist.

242 The ^{14}C -RO content decreased exponentially with increasing temperature (Fig. 2), implying that the
243 CO_2 evolved from labile (low temperature) OC had a greater ^{14}C content than the CO_2 evolved from
244 recalcitrant (high temperature) OC. Since the ^{14}C content of all RO fractions was $<100\%$ Modern (Fig.
245 2 Table 1), each of the OC reactivity pools were likely to be predominantly composed of carbon
246 sequestered from the atmosphere before the 1963 ^{14}C bomb-spike caused by atmospheric nuclear
247 weapons testing, although we cannot completely discount some contributions from post-bomb
248 carbon (Hajdas et al., 2021). Nevertheless, using ^{14}C content as an estimate of the age of the OC we
249 can infer that carbon reactivity decreases with increasing age for these samples. This finding is
250 consistent with previous studies on the thermal reactivity of carbon stored in soils and sediments
251 (Bao et al., 2019; Luk et al., 2021; Plante et al., 2013; Stoner et al., 2023).

252 The results suggest inhomogeneity within at least one of the temperature fractions for each sample
253 as, although there were no post-bomb ^{14}C contents for the incubation or RO samples (Table 1), there
254 is likely to be a fraction of post-bomb (post-AD1955) OC in at least one of the temperature fractions.
255 This is due to autochthonous OC sequestration at this accreting saltmarsh (Hajdas et al., 2021;
256 Smeaton et al., 2024) which may become obscured by contributions from pre-bomb OC. Observing
257 the exponential decline in ^{14}C content with increasing temperature (Fig. 2), we hypothesise that, if
258 present, this mixing of pre- and post-bomb C most likely occurred in the 150-325°C fraction. As ^{14}C
259 content decreases with increasing temperature for the RO fractions, CO_2 with ^{14}C content greater
260 than any of the measured RO fractions would be expected to have been evolved within the lowest
261 temperature fraction (150-325°C).

262 The ^{14}C -RO contents ranged from $97.53 \pm 0.50\%$ Modern for T2 15.5 cm in the 150-325°C fraction to
263 $15.70 \pm 0.12\%$ Modern for T1 18.5 cm (Table 1), highlighting the role of saltmarshes both as stores of
264 contemporary and highly aged carbon as these ^{14}C contents correspond to
265 conventional radiocarbon years BP (relative to AD 1950) of 201 ± 41 years BP and $14,875 \pm 61$
266 years BP, respectively (Table A2). While regional deglaciation of this part of Scotland is likely to
267 postdate the age of $14,875 \pm 61$ years BP (Ballantyne and Small, 2019), we note that the catchment
268 geology contains sources of petrogenic carbon (Miller et al., 2023), which would be ^{14}C -dead and
269 may have diluted the ^{14}C content of the highest temperature RO- CO_2 fractions. As the oldest carbon
270 was stored in the lowest reactivity fraction (Fig. 2), this emphasises that saltmarshes accumulating



271 greater amounts of pre-aged OC will likely provide the most stable OC stores, and saltmarshes
272 accumulating greater proportions of contemporary OC, either through in-situ production or young
273 allochthonous components, contain soil OC stores which are of greater vulnerability for
274 remineralisation and loss to the atmosphere (Komada et al., 2022; Van de Broek et al., 2018).
275 However, the ^{14}C contents of the 150-325°C fraction (81-98 % Modern) correspond to uncalibrated
276 ^{14}C ages of 201 - 1643 years BP (SI), highlighting that although OC reactivity decreases with age (Fig.
277 2), the labile OC fraction can still be centuries to millennia in age for these soils and that, due to the
278 often anaerobic and non-eroding conditions of buried sediments, saltmarshes can be stores of old,
279 but reactive, carbon.

280 **4.3. ^{13}C content of ramped oxidation CO_2 fractions**

281 ^{13}C -RO also had a significant trend with temperature, increasing linearly (Fig. 3). Therefore, thermally
282 recalcitrant OC (oxidised at high temperatures) tended to be ^{13}C enriched compared to labile OC.
283 This implies that the recalcitrant OC was likely to be composed of a greater amount of OC which has
284 undergone microbial decomposition as this process tends to enrich the degraded OC in ^{13}C (Boström
285 et al., 2007; Etcheverría et al., 2009; Luk et al., 2021; Sanderman & Grandy, 2020; Soldatova et al.,
286 2024; Stoner et al., 2023). It is also possible that methodological artefacts, such as kinetic
287 fractionation, influenced the ^{13}C -RO contents. Kinetic fractionation is explained by different carbon
288 isotopes evolving as CO_2 from the soil sample at different rates during the ramped heating
289 (Hemingway et al., 2017). Kinetic fractionation would cause the ^{13}C content of the evolved CO_2 to
290 increase linearly with temperature (Hemingway et al., 2017), as we observed in Fig. 3, so we cannot
291 rule out this artefact.

292 The range in ^{13}C -RO contents between 150-800°C shows a clear distinction between 150-650°C and
293 650-800°C (Table 2). There was a strong positive linear relationship between ^{13}C content and
294 temperature for the 150-650°C range (Fig. 3), which was not the case for the 650-800°C range as the
295 ^{13}C contents of the CO_2 evolved from the 500-650°C to the 650-800°C range increases in a non-linear
296 manner (Table 2). This is likely to be because the C pools from 150-650°C are mostly composed of
297 OC, whereas the 650-800°C pool is mostly composed of IC. We deemed this to be the case as the
298 ^{13}C contents of the CO_2 evolved between 150-650°C were typical of OC sources (Leng et al., 2006;
299 Leng & Lewis, 2017), whereas the ^{13}C contents of the CO_2 evolved between 650-800°C were mostly
300 typical of at least a partial contribution from an IC source, with the exception of T2 5.5 cm and T3 5.5
301 cm (Table 2) (Brand et al., 2014; Ramnarine et al., 2012).



302 The CO₂ evolved from 650-800°C for T1 0.5 cm had a ¹³C content of -5.6 ‰, indicating that it was from
303 a predominantly IC source. Given the ¹⁴C content was 79.75 ± 0.37 % Modern, we determined that
304 this was likely to be from a biogenic IC source, potentially shell fragments.

305 **4.4. Comparison of biologically and thermally evolved CO₂**

306 For these saltmarsh soils, thermally recalcitrant OC was ¹³C-enriched and ¹⁴C-depleted compared
307 to thermally labile OC. This implies that labile OC tends to be relatively young compared to
308 recalcitrant OC which tends to be composed of more degraded and aged OC. These findings are
309 consistent with a previous study on the thermal reactivity (using ramped pyrolysis oxidation) of
310 saltmarsh soil OM (Luk et al., 2021) and other soil and sediment OM studies (Sanderman and Grandy,
311 2020; Stoner et al., 2023).

312 We did not attempt to relate the ¹³C-RO to the ¹³C content of the CO₂ respired in the incubation
313 experiments, due to the potential for microbial fractionation during the incubation experiments.
314 Microbial alteration can change the ¹³C content of the respired CO₂ and the resulting soil OC
315 (Soldatova et al., 2024; Werth and Kuzyakov, 2010), so it is possible that the CO₂ collected for isotopic
316 analysis in Houston et al. (2024) did not reflect the ¹³C content of the OC pool it was respired from.
317 Therefore, the ¹³C content of the biologically evolved CO₂ and the ¹³C-RO measured in this study are
318 not comparable. We focus the remainder of our discussion on comparing the ¹⁴C content of the
319 biologically evolved CO₂ (Houston et al., 2024) to ¹⁴C-RO measured in this study, which would not be
320 affected by microbial fractionation during the incubation period (¹⁴C results are normalised using the
321 measured δ¹³C values and therefore corrected for isotopic fractionation).

322 Fig. 4 shows that for each of the 0.5 cm depth samples, the ¹⁴C content of the CO₂ respired in the
323 aerobic laboratory experiments was ¹⁴C-enriched relative to any of the RO temperature fractions,
324 which was also the case for the T3 5.5 cm sample (Table 1). This was likely to be caused by
325 inhomogeneity in the OC reactivity pools, as each defined thermal reactivity pool may be composed
326 of multiple OC sources of variable age and composition. Due to the negative exponential relationship
327 between ¹⁴CO₂-RO and temperature (Fig. 2), we hypothesise that for soil samples producing respired
328 CO₂ that was ¹⁴C-enriched relative to any of the RO fractions (T1 0.5 cm, T2 0.5 cm, T3 0.5 cm, T3 5.5
329 cm; Table 1, Fig. 4), that this CO₂ was biologically-produced from an OC pool within the most
330 thermally labile RO fraction (150-325°C). Thus, we suggest that even within the 150-325 °C RO
331 fraction there are pools of even younger OM, but that they are masked by older, ¹⁴C-depleted OM.



332 This implies that RO-¹⁴C analysis of finer temperature fractions could provide further insights into the
333 turnover of young carbon in these soils.

334 The ¹⁴C content of respired CO₂ from the 5.5 cm depth samples tended to be closer to the ¹⁴C content
335 of the lowest temperature (150-325°C) RO fraction (Fig. 4), implying that for these samples the
336 biologically evolved CO₂ was from a thermally labile OC pool. The T2 15.5 cm respired CO₂ sample
337 was also similar in ¹⁴C content to the lowest temperature RO fraction, whereas respired CO₂ from the
338 slightly deeper T1 18.5 cm and T3 19.5 cm samples was ¹⁴C-depleted relative to the 150-325°C RO
339 fraction, instead aligning closer to the higher temperature RO fractions (Fig. 4). This implies that the
340 biologically evolved CO₂ from T1 18.5 cm and T3 19.5 cm was not from a thermally labile OC pool.
341 The ¹⁴C content of the CO₂ evolved from the aerobic incubations of T1 18.5 cm and T3 19.5 cm was
342 hypothesized to have been evolved from an inorganic C source due to the enriched ¹³C contents of -
343 6.1‰ and -3.7‰, respectively (Houston et al., 2024). As IC reactivity is controlled by different factors
344 than OC reactivity (Van Dam et al., 2021), and the remainder of the samples were determined to
345 evolve from OC substrates, this is likely to explain why the ¹⁴C content of the CO₂ evolved from the
346 aerobic incubation experiments for T1 18.5 cm and T3 19.5 cm did not align with the lowest
347 temperature (most thermally labile) RO fraction (Fig. 4). Therefore, there was a clear depth trend in
348 the relationship between the ¹⁴C content of CO₂ respired in the aerobic incubation experiments and
349 the ¹⁴C content of the CO₂ evolved during RO of the same bulk soils.

350 The depleted ¹⁴C contents of some of the OC accumulating at the Skinflats saltmarsh (201 ± 41 years
351 BP to 14,875 ± 61 years BP; Table A2) imply that a proportion of the OC being buried may have been
352 pre-aged at the time of deposition on the marsh surface, as the marsh formed in the 1930's (Miller et
353 al., 2023). This means that some of the OC may have undergone significant microbial processing and
354 degradation prior to its accumulation in the saltmarsh soil. It is also possible that highly aged OC
355 could remain labile if it had been stored in an environment with low rates of microbial decomposition,
356 e.g., a peatland (Dean et al., 2023). Regardless of the age and degradation state of the OC deposited
357 onto the marsh surface, as it gets buried it will undergo a degree of microbial processing and
358 degradation in the saltmarsh soil (Luk et al., 2021). As the OM is degraded, and the energetically
359 favourable components are consumed, the resulting OM becomes increasingly recalcitrant (Luk et
360 al., 2021; Sanderman and Grandy, 2020; Soldatova et al., 2024). Therefore, at depth we would expect
361 to see an increase in the relative proportion of recalcitrant OC, which we do for T1 and T3 (Fig. 1). The
362 in-situ degradation of soil OM may reduce these inhomogeneities with depth as the labile OM



363 components either get consumed or degraded to a recalcitrant (higher RO temperature) state. We
364 did not measure fine-scale changes in RO-¹⁴C content within the 150-325°C temperature window for
365 any of the samples, but if this is the case, there would be less of a range of ¹⁴C contents within the
366 150-325°C RO fraction for the 5.5 cm and deeper samples than for the 0.5 cm samples

367 For seven out of nine samples (T1 18.5 cm and T3 19.5 cm being the outliers), the ¹⁴C content of the
368 CO₂ evolved from the aerobic laboratory incubations was closest to the ¹⁴C content of the 150-325°C
369 RO temperature fraction. Therefore, even though the CO₂ evolved from the aerobic incubation
370 experiments was determined to be from a predominantly aged, allochthonous OC source (Houston
371 et al., 2024), it can now also be shown to be derived from a predominantly thermally labile OC pool
372 (Fig. 4). The results from our study suggest that saltmarshes can be stores of old, labile OC which is
373 vulnerable to remineralisation and loss to the atmosphere in oxic conditions, e.g. when a saltmarsh
374 is drained or the soils disturbed.

375 5. Conclusions

376 This is the first study on saltmarsh soils to employ the ramped oxidation method. We show that ¹⁴C-
377 depleted (up to 14,875 years BP) carbon dominates the recalcitrant OC pools, whereas the labile OC
378 pools are composed of younger (201-1843 years BP) carbon. These results highlight the role of
379 saltmarshes as stores of both old, recalcitrant OC, as well as old, labile OC.

380 We present the first comparison of the bioavailability (CO₂ evolved from incubation experiments;
381 Houston et al., 2024) and the thermal reactivity (RO) of saltmarsh soil OC. We show that pre-aged
382 CO₂ evolved from saltmarsh soils exposed to oxic conditions (Houston et al., 2024) are from a
383 predominantly labile OC pool. As saltmarsh soils exist mostly in low oxygen, waterlogged conditions,
384 management interventions to limit their exposure to elevated oxygen availability may protect and
385 conserve these stores of old, labile OC and provide a climate abatement service.

386 Appendix A

387 *Table A1. Percentage of CO₂ evolved during ramped oxidation of each sample from the labile (150-425°C) and recalcitrant*
388 *388 (425-650°C) temperature ranges.*

	Labile (150-425°C)	Recalcitrant (425-650°C)
T1 0.5 cm	59.54	40.46
T1 5.5 cm	62.99	37.01
T1 18.5 cm	60.12	39.88
T2 0.5 cm	57.53	42.47



T2 5.5 cm	50.00	50.00
T2 15.5 cm	64.07	35.93
T3 0.5 cm	64.97	35.03
T3 5.5 cm	59.61	40.39
T3 19.5 cm	64.86	35.14

389

390 *Table A2. Conventional radiocarbon age (years BP, where 0 BP = AD 1950 and age = $-8033 \times \ln(\%Modern/100)$) for each of*
 391 *the samples. Measurement errors are reported to one standard deviation (1σ). We also report the amount of CO₂ evolved*
 392 *from each temperature fraction from which CO₂ was collected for ¹⁴C measurement, reported as %Carbon.*

	Radiocarbon Age (years BP)	Radiocarbon Age 1σ uncertainty	%Carbon
T1 0.5 cm 150-325°C	1,341	42	1.42
T1 0.5 cm 325-425°C	4,800	43	1.17
T1 0.5 cm 425-500°C	7,527	42	1.07
T1 0.5 cm 500-650°C	6,108	44	0.69
T1 0.5 cm 650-800°C	1,818	37	0.53
T1 5.5 cm 150-325°C	1,072	40	1.44
T1 5.5 cm 325-425°C	4,740	41	1.59
T1 5.5 cm 425-500°C	10,011	46	1.11
T1 5.5 cm 500-650°C	10,650	48	0.67
T1 18.5 cm 150-325°C	1,347	42	1.48
T1 18.5 cm 325-425°C	6,769	43	1.43
T1 18.5 cm 425-500°C	12,900	53	1.31
T1 18.5 cm 500-650°C	14,875	61	0.62
T2 0.5 cm 150-325°C	1,643	42	1.45
T2 0.5 cm 325-425°C	6,230	42	1.30
T2 0.5 cm 425-500°C	13,924	58	1.44
T2 0.5 cm 500-650°C	12,826	55	0.59
T2 5.5 cm 150-325°C	851	38	1.09
T2 5.5 cm 325-425°C	4,030	40	1.13
T2 5.5 cm 425-500°C	9,528	43	1.12
T2 5.5 cm 500-650°C	14,184	56	1.10
T2 15.5 cm 150-325°C	201	41	2.66



T2 15.5 cm 325-425°C	1,813	41	2.60
T2 15.5 cm 425-500°C	3,640	40	2.12
T2 15.5 cm 500-650°C	4,956	40	0.83
T3 0.5 cm 150-325°C	1,085	41	1.98
T3 0.5 cm 325-425°C	5,086	42	1.60
T3 0.5 cm 425-500°C	10,707	47	1.38
T3 0.5 cm 500-650°C	9,794	45	0.55
T3 5.5 cm 150-325°C	1,190	39	1.13
T3 5.5 cm 325-425°C	5,591	41	1.32
T3 5.5 cm 425-500°C	12,211	52	1.08
T3 5.5 cm 500-650°C	13,617	54	0.58
T3 19.5 cm 150-325°C	1,379	39	1.48
T3 19.5 cm 325-425°C	7,033	43	1.75
T3 19.5 cm 425-500°C	13,322	55	1.11
T3 19.5 cm 500-650°C	13,026	55	0.64

393

394 **Data Availability**

395 All data presented in this manuscript is available in the main text, appendices, and supporting
396 information.

397 **Author Contribution Statement**

398 A.H. undertook the study, fieldwork, sample processing, data acquisition, and wrote the first draft of
399 the manuscript. M.G. conducted the laboratory procedures with the help of A.H. A.H., W.A., and M.G.
400 contributed to designing the study, fieldwork, and laboratory analyses. W.A., M.G., and J.S. oversaw
401 the study and contributed to writing and revision of the manuscript.

402 **Competing Interests**

403 The authors declare that they have no conflict of interest.

404 **Acknowledgements**

405 We thank the NERC SUPER DTP for funding the PhD through which this research was undertaken
406 (NE/S007342/1). We acknowledge support from the National Environmental Isotope Facility in



407 funding the ^{14}C measurements for this study under grant NE/S011587/1 (allocation numbers
408 2594.1022, 2709.1023). WA also acknowledges support provided by the HORIZON-CL5-2023-D1-02-
409 02 grant C-BLUES, Innovation to advance the evidence base for reporting of Blue Carbon inventories
410 and greenhouse gas fluxes in coastal wetlands. Finally, thanks are extended to Chloe Bates for
411 assisting with sample collection.

412 **References**

- 413 Ballantyne, C. K. and Small, D.: The Last Scottish Ice Sheet, *Earth and Environmental Science*
414 *Transactions of The Royal Society of Edinburgh*, 110, 93–131,
415 <https://doi.org/10.1017/S1755691018000038>, 2019.
- 416 Bao, R., Zhao, M., McNichol, A., Wu, Y., Guo, X., Haghypour, N., and Eglinton, T. I.: On the Origin of
417 Aged Sedimentary Organic Matter Along a River-Shelf-Deep Ocean Transect, *Journal of Geophysical*
418 *Research: Biogeosciences*, 124, 2582–2594, <https://doi.org/10.1029/2019JG005107>, 2019.
- 419 Bernal, B., Megonigal, J. P., and Mozdzer, T. J.: An invasive wetland grass primes deep soil carbon
420 pools, *Global Change Biology*, 23, 2104–2116, <https://doi.org/10.1111/gcb.13539>, 2017.
- 421 Boström, B., Comstedt, D., and Ekblad, A.: Isotope fractionation and ^{13}C enrichment in soil
422 profiles during the decomposition of soil organic matter, *Oecologia*, 153, 89–98,
423 <https://doi.org/10.1007/s00442-007-0700-8>, 2007.
- 424 Brand, W. A., Coplen, T. B., Vogl, J., Rosner, M., and Prohaska, T.: Assessment of international
425 reference materials for isotope-ratio analysis (IUPAC Technical Report), *Pure and Applied*
426 *Chemistry*, 86, 425–467, <https://doi.org/10.1515/pac-2013-1023>, 2014.
- 427 Capel, E. L., de la Rosa Arranz, J. M., González-Vila, F. J., González-Perez, J. A., and Manning, D. A.
428 C.: Elucidation of different forms of organic carbon in marine sediments from the Atlantic coast of
429 Spain using thermal analysis coupled to isotope ratio and quadrupole mass spectrometry, *Organic*
430 *Geochemistry*, 37, 1983–1994, <https://doi.org/10.1016/j.orggeochem.2006.07.025>, 2006.
- 431 Chapman, S. K., Hayes, M. A., Kelly, B., and Langley, J. A.: Exploring the oxygen sensitivity of
432 wetland soil carbon mineralization, *Biology Letters*, 15, 20180407,
433 <https://doi.org/10.1098/rsbl.2018.0407>, 2019.



- 434 Dasari, S., Garnett, M. H., and Hilton, R. G.: Leakage of old carbon dioxide from a major river system
435 in the Canadian Arctic, *PNAS Nexus*, 3, pgae134, <https://doi.org/10.1093/pnasnexus/pgae134>,
436 2024.
- 437 Dean, J. F., Billett, M. F., Turner, T. E., Garnett, M. H., Andersen, R., McKenzie, R. M., Dinsmore, K. J.,
438 Baird, A. J., Chapman, P. J., and Holden, J.: Peatland pools are tightly coupled to the contemporary
439 carbon cycle, *Global Change Biology*, n/a, e16999, <https://doi.org/10.1111/gcb.16999>, 2023.
- 440 Etcheverría, P., Huygens, D., Godoy, R., Borie, F., and Boeckx, P.: Arbuscular mycorrhizal fungi
441 contribute to ^{13}C and ^{15}N enrichment of soil organic matter in forest soils, *Soil Biology and*
442 *Biochemistry*, 41, 858–861, <https://doi.org/10.1016/j.soilbio.2009.01.018>, 2009.
- 443 Garnett, M. H., Pereira, R., Taylor, C., Murray, C., and Ascough, P. L.: A NEW RAMPED OXIDATION-
444 ^{14}C ANALYSIS FACILITY AT THE NEIF RADIOCARBON LABORATORY, EAST KILBRIDE, UK,
445 *Radiocarbon*, 65, 1213–1229, <https://doi.org/10.1017/RDC.2023.96>, 2023.
- 446 Granse, D., Wanner, A., Stock, M., Jensen, K., and Mueller, P.: Plant-sediment interactions decouple
447 inorganic from organic carbon stock development in salt marsh soils, *Limnology and Oceanography*
448 *Letters*, n/a, <https://doi.org/10.1002/lol2.10382>, 2024.
- 449 Hajdas, I., Ascough, P., Garnett, M. H., Fallon, S. J., Pearson, C. L., Quarta, G., Spalding, K. L.,
450 Yamaguchi, H., and Yoneda, M.: Radiocarbon dating, *Nat Rev Methods Primers*, 1, 1–26,
451 <https://doi.org/10.1038/s43586-021-00058-7>, 2021.
- 452 Hemingway, J. D., Galy, V. V., Gagnon, A. R., Grant, K. E., Rosengard, S. Z., Soulet, G., Zigah, P. K.,
453 and McNichol, A. P.: Assessing the Blank Carbon Contribution, Isotope Mass Balance, and Kinetic
454 Isotope Fractionation of the Ramped Pyrolysis/Oxidation Instrument at NOSAMS, *Radiocarbon*, 59,
455 179–193, <https://doi.org/10.1017/RDC.2017.3>, 2017.
- 456 Houston, A., Garnett, M. H., and Austin, W. E. N.: Blue carbon additionalty: New insights from the
457 radiocarbon content of saltmarsh soils and their respired CO_2 , *Limnology and Oceanography*, n/a,
458 <https://doi.org/10.1002/lno.12508>, 2024.
- 459 Howard, J., Sutton-Grier, A. E., Smart, L. S., Lopes, C. C., Hamilton, J., Kleypas, J., Simpson, S.,
460 McGowan, J., Pessarrodona, A., Alleway, H. K., and Landis, E.: Blue carbon pathways for climate



- 461 mitigation: Known, emerging and unlikely, *Marine Policy*, 156, 105788,
462 <https://doi.org/10.1016/j.marpol.2023.105788>, 2023.
- 463 Komada, T., Bravo, A., Brinkmann, M.-T., Lu, K., Wong, L., and Shields, G.: “Slow” and “fast” in blue
464 carbon: Differential turnover of allochthonous and autochthonous organic matter in minerogenic
465 salt marsh sediments, *Limnology and Oceanography*, n/a, <https://doi.org/10.1002/lno.12090>, 2022.
- 466 Leng, M. J. and Lewis, J. P.: C/N ratios and Carbon Isotope Composition of Organic Matter in
467 Estuarine Environments, in: *Applications of Paleoenvironmental Techniques in Estuarine Studies*,
468 edited by: Weckström, K., Saunders, K. M., Gell, P. A., and Skilbeck, C. G., Springer Netherlands,
469 Dordrecht, 213–237, https://doi.org/10.1007/978-94-024-0990-1_9, 2017.
- 470 Leng, M. J., Lamb, A. L., Heaton, T. H. E., Marshall, J. D., Wolfe, B. B., Jones, M. D., Holmes, J. A., and
471 Arrowsmith, C.: Isotopes in Lake Sediments, in: *Isotopes in Palaeoenvironmental Research*, edited
472 by: Leng, M. J., Springer Netherlands, Dordrecht, 147–184, [https://doi.org/10.1007/1-4020-2504-](https://doi.org/10.1007/1-4020-2504-1_04)
473 [1_04](https://doi.org/10.1007/1-4020-2504-1_04), 2006.
- 474 Leorri, E., Zimmerman, A. R., Mitra, S., Christian, R. R., Fatela, F., and Mallinson, D. J.: Refractory
475 organic matter in coastal salt marshes-effect on C sequestration calculations, *Science of the Total*
476 *Environment*, 633, 391–398, <https://doi.org/10.1016/j.scitotenv.2018.03.120>, 2018.
- 477 Luk, S. Y., Todd-Brown, K., Eagle, M., McNichol, A. P., Sanderman, J., Gosselin, K., and Spivak, A. C.:
478 Soil Organic Carbon Development and Turnover in Natural and Disturbed Salt Marsh Environments,
479 *Geophysical Research Letters*, 48, e2020GL090287, <https://doi.org/10.1029/2020GL090287>, 2021.
- 480 Macreadie, P. I., Anton, A., Raven, J. A., Beaumont, N., Connolly, R. M., Friess, D. A., Kelleway, J. J.,
481 Kennedy, H., Kuwae, T., Lavery, P. S., Lovelock, C. E., Smale, D. A., Apostolaki, E. T., Atwood, T. B.,
482 Baldock, J., Bianchi, T. S., Chmura, G. L., Eyre, B. D., Fourqurean, J. W., Hall-Spencer, J. M., Huxham,
483 M., Hendriks, I. E., Krause-Jensen, D., Laffoley, D., Luisetti, T., Marbà, N., Masque, P., McGlathery, K.
484 J., Megonigal, J. P., Murdiyarsa, D., Russell, B. D., Santos, R., Serrano, O., Silliman, B. R., Watanabe,
485 K., and Duarte, C. M.: The future of Blue Carbon science, *Nature Communications*, 10, 3998,
486 <https://doi.org/10.1038/s41467-019-11693-w>, 2019.



- 487 Macreadie, P. I., Costa, M. D. P., Atwood, T. B., Friess, D. A., Kelleway, J. J., Kennedy, H., Lovelock, C.
488 E., Serrano, O., and Duarte, C. M.: Blue carbon as a natural climate solution, *Nat Rev Earth Environ*,
489 2, 826–839, <https://doi.org/10.1038/s43017-021-00224-1>, 2021.
- 490 McTigue, N. D., Walker, Q. A., and Currin, C. A.: Refining Estimates of Greenhouse Gas Emissions
491 From Salt Marsh “Blue Carbon” Erosion and Decomposition, *Frontiers in Marine Science*, 8, 2021.
- 492 Miller, L. C., Smeaton, C., Yang, H., and Austin, W. E. N.: Carbon accumulation and storage across
493 contrasting saltmarshes of Scotland, *Estuarine, Coastal and Shelf Science*, 108223,
494 <https://doi.org/10.1016/j.ecss.2023.108223>, 2023.
- 495 Mueller, P., Do, H. T., Jensen, K., and Nolte, S.: Origin of organic carbon in the topsoil of Wadden Sea
496 salt marshes, *Marine Ecology Progress Series*, 624, 39–50, <https://doi.org/10.3354/meps13009>,
497 2019.
- 498 Noyce, G. L., Smith, A. J., Kirwan, M. L., Rich, R. L., and Megonigal, J. P.: Oxygen priming induced by
499 elevated CO₂ reduces carbon accumulation and methane emissions in coastal wetlands, *Nat.*
500 *Geosci.*, 16, 63–68, <https://doi.org/10.1038/s41561-022-01070-6>, 2023.
- 501 Peltre, C., Fernández, J. M., Craine, J. M., and Plante, A. F.: Relationships between Biological and
502 Thermal Indices of Soil Organic Matter Stability Differ with Soil Organic Carbon Level, *Soil Science*
503 *Society of America Journal*, 77, 2020–2028, <https://doi.org/10.2136/sssaj2013.02.0081>, 2013.
- 504 Plante, A. F., Fernández, J. M., and Leifeld, J.: Application of thermal analysis techniques in soil
505 science, *Geoderma*, 153, 1–10, <https://doi.org/10.1016/j.geoderma.2009.08.016>, 2009.
- 506 Plante, A. F., Fernández, J. M., Haddix, M. L., Steinweg, J. M., and Conant, R. T.: Biological, chemical
507 and thermal indices of soil organic matter stability in four grassland soils, *Soil Biology and*
508 *Biochemistry*, 43, 1051–1058, <https://doi.org/10.1016/j.soilbio.2011.01.024>, 2011.
- 509 Plante, A. F., Beaupré, S. R., Roberts, M. L., and Baisden, T.: Distribution of Radiocarbon Ages in Soil
510 Organic Matter by Thermal Fractionation, *Radiocarbon*, 55, 1077–1083,
511 <https://doi.org/10.1017/S0033822200058215>, 2013.
- 512 Ramnarine, R., Wagner-Riddle, C., Dunfield, K. E., and Voroney, R. P.: Contributions of carbonates
513 to soil CO₂ emissions, *Can. J. Soil. Sci.*, 92, 599–607, <https://doi.org/10.4141/cjss2011-025>, 2012.



- 514 Rumpel, C. and Kögel-Knabner, I.: Deep soil organic matter—a key but poorly understood
515 component of terrestrial C cycle, *Plant Soil*, 338, 143–158, [https://doi.org/10.1007/s11104-010-](https://doi.org/10.1007/s11104-010-0391-5)
516 0391-5, 2011.
- 517 Saintilan, N., Rogers, K., Mazumder, D., and Woodroffe, C.: Allochthonous and autochthonous
518 contributions to carbon accumulation and carbon store in southeastern Australian coastal
519 wetlands, *Estuarine, Coastal and Shelf Science*, 128, 84–92,
520 <https://doi.org/10.1016/j.ecss.2013.05.010>, 2013.
- 521 Sanderman, J. and Grandy, A. S.: Ramped thermal analysis for isolating biologically meaningful soil
522 organic matter fractions with distinct residence times, *SOIL*, 6, 131–144,
523 <https://doi.org/10.5194/soil-6-131-2020>, 2020.
- 524 Smeaton, C., Garrett, E., Koot, M. B., Ladd, C. J. T., Miller, L. C., McMahon, L., Foster, B., Barlow, N.
525 L. M., Blake, W., Gehrels, W. R., Skov, M. W., and Austin, W. E. N.: Organic carbon accumulation in
526 British saltmarshes, *Science of The Total Environment*, 926, 172104,
527 <https://doi.org/10.1016/j.scitotenv.2024.172104>, 2024.
- 528 Soldatova, E., Krasilnikov, S., and Kuzyakov, Y.: Soil organic matter turnover: Global implications
529 from $\delta^{13}\text{C}$ and $\delta^{15}\text{N}$ signatures, *Science of The Total Environment*, 912, 169423,
530 <https://doi.org/10.1016/j.scitotenv.2023.169423>, 2024.
- 531 Stoner, S. W., Schrumpf, M., Hoyt, A., Sierra, C. A., Doetterl, S., Galy, V., and Trumbore, S.: How well
532 does ramped thermal oxidation quantify the age distribution of soil carbon? Assessing thermal
533 stability of physically and chemically fractionated soil organic matter, *Biogeosciences*, 20, 3151–
534 3163, <https://doi.org/10.5194/bg-20-3151-2023>, 2023.
- 535 Van Dam, B. R., Zeller, M. A., Lopes, C., Smyth, A. R., Böttcher, M. E., Osburn, C. L., Zimmerman, T.,
536 Pröfrock, D., Fourqurean, J. W., and Thomas, H.: Calcification-driven CO₂ emissions exceed “Blue
537 Carbon” sequestration in a carbonate seagrass meadow, *Science Advances*, 7, eabj1372,
538 <https://doi.org/10.1126/sciadv.abj1372>, 2021.
- 539 Van de Broek, M., Vandendriessche, C., Poppelmonde, D., Merckx, R., Temmerman, S., and Govers,
540 G.: Long-term organic carbon sequestration in tidal marsh sediments is dominated by old-aged



- 541 allochthonous inputs in a macrotidal estuary, *Global Change Biology*, 24, 2498–2512,
542 <https://doi.org/10.1111/gcb.14089>, 2018.
- 543 Werth, M. and Kuzyakov, Y.: 13C fractionation at the root–microorganisms–soil interface: A review
544 and outlook for partitioning studies, *Soil Biology and Biochemistry*, 42, 1372–1384,
545 <https://doi.org/10.1016/j.soilbio.2010.04.009>, 2010.
- 546 Williams, E. K. and Plante, A. F.: A Bioenergetic Framework for Assessing Soil Organic Matter
547 Persistence, *Frontiers in Earth Science*, 6, 2018.
- 548